Reaction intermediate species during the steam reforming of methanol over metal modified molybdenum carbide catalysts

Ji Cao [a,1], Yufei Ma [a,1], Guoqing Guan [a,b,*], Xiaogang Hao [c], Xuli Ma [b,c], Zhongde Wang [c], Katsuki Kusakabe [d], Abuliti Abudula [a,b]

[a] Graduate School of Science and Technology, Hirosaki University, 3 Bunkyo-cho, Hirosaki, Aomori 036-8561, Japan
[b] North Japan Research Institute for Sustainable Energy, Hirosaki University, 2-1-3 Matsubara, Aomori 030-0813, Japan
[c] Department of Chemical Engineering, Taiyuan University of Technology, Taiyuan 030024, China
[d] Department of Nanoscience, Sojo University, 4-22-1 Ikeda, Kumamoto 860-0082, Japan

ABSTRACT

To understand steam reforming of methanol (SRM) reaction pathways over the surfaces of various metal-modified molybdenum carbides, the reaction intermediate species generated during the SRM reaction are investigated by using a temperature programmed surface reaction (TPSR) approach, in which a mass spectroscopy is applied to detect the produced species on-line. It is found that the reaction temperature affects the formation of different intermediate species over different catalysts. At the temperature lower than 180 °C, SRM reaction proceeds over Cu modified molybdenum carbide surface through formic acid (HCOOH) intermediate pathway, but at the temperature over 180 °C, the reactions over pure β-Mo_2C, Ni, Cu and Pt modified molybdenum carbide surfaces proceed through methyl-formate ($HCOOCH_3$) intermediate pathway. It is expected that these findings can help us to understand the mechanism on SRM reaction over molybdenum carbide based catalysts.

© 2016 Elsevier B.V. All rights reserved.

1. Introduction

Compared with gaseous hydrogen storage, on-board hydrogen production by reforming liquid hydrogen carriers will be more potential for future commercialization. Steam reforming of methanol (SRM) is considered as one of the most favorable chemical processes for on-board hydrogen production because: (i) methanol is in liquid state at ambient condition; (ii) it has high hydrogen-to-carbon ratio; (iii) the activation of methanol can occur at low temperatures (200–400 °C); (iv) methanol is sulfur free and can be produced from biomass [1].

Various catalysts have been developed for the SRM [1–10]. Cu-based catalyst is widely used for SRM reaction due to its high activity and high selectivity at low temperature. However, this kind of catalyst is easy to be deactivated by thermal sintering [1–5]. Group 8–10 catalysts have also been developed for the SRM with high activity and stability, but their performances are generally affected by the support. Noble metals like Pt, Pd and Au

supported oxides generally shows high activity, stability and selectivity [7–10], but their cost hinders their large scale applications. In our previous studies [11–14], metal-modified molybdenum carbide catalysts were prepared for low-temperature SRM reaction. It is found that the activation of methanol molecule can be promoted by the loading of metal (Fe, Co, Ni, Cu or Pt) on the molybdenum carbide, and water molecule is mainly activated on molybdenum carbide surface itself. By adjusting the molar ratio of metal to carbide, the catalytic activity and stability can be tuned. Moreover, surface oxidation is usually the main reason for deactivation of carbide catalysts [11–25].

Three different reaction pathways for the SRM reaction over catalyst have been proposed in the literature [26–32]. The first one is the methanol decomposition to H_2 and CO followed by water gas shift (WGS) reaction (Pathway I, CO intermediate); the second one is methanol dehydrogenation to methyl-formate, which then further decomposed to H_2 and CO_2 (Pathway II); and the third one is the methanol dehydrogenation to formaldehyde followed by decomposition to final products (Pathway III). These three pathways are summarized as the followings.
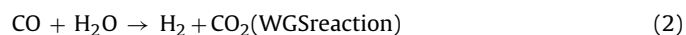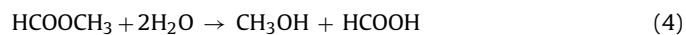
Pathway I (CO intermediate):

$$CH_3OH \rightarrow 2H_2 + CO \quad (1)$$

$$CO + H_2O \rightarrow H_2 + CO_2 (WGS \, reaction) \qquad (2)$$

Pathway II (Methyl-formate intermediate):

$$2CH_3OH \rightarrow HCOOCH_3 + 2H_2 \qquad (3)$$

$$HCOOCH_3 + 2H_2O \rightarrow CH_3OH + HCOOH \qquad (4)$$

$$HCOOH \rightarrow H_2 + CO_2 \qquad (5)$$

Pathway III (Formaldehyde intermediate):

$$CH_3OH \rightarrow HCHO + H_2 \qquad (6)$$

$$HCHO + H_2O \rightarrow HCOOH + H_2 \qquad (7)$$

$$HCOOH \rightarrow H_2 + CO_2 \qquad (8)$$

For the pathway I, CO is the primary product. Based on thermodynamic condition of WGS reaction, CO concentration should be at least equal to or higher than the H_2O concentration. However, Santacesaria and Carra [26] studied the SRM reation over Cu-Zn catalyts in a continuous strired-tank reactor (CSTR) using Langmuir-Hinshelwood model, and found that CO concentration was lower than the equilibrium concentration of WGS rection. Luo and Asthagiri [27] applied density functional theory (DFT) to study the SRM reaction on Co (001) and Co (111) surface and found that CO cannot be obtained from the direct decomposion of methanol, but from the decomposition of CH_2O which is generated by methanol dehydrogenation. These results indicate that the pathway I is doubtful. For the pathway I, based on the diffuse reflectance infrared fourier transform (DRIFT) spectroscopic results, Frank et al. [28] found that methyl-formate was the intermediate species in SRM reaction over Cu-based catalysts. Furthermore, according to plane-wave density functional theory, Lin et al. [29] considered that the methy formate intermediate should be formed by a reaction between formaldehyde and methoxyl. Yi et al. [30] identified the pathway II occurring on the Au/CeO_2 surface via in-situ temperature program surface reaction (TPSR) approach. For the pathway III, Takezawa and Iwasa [31] found that formaldehyde (HCHO) is an important intermediate involved in the SRM reaction over Cu and group VIII (Ni, Rh, Pd and Pt) metal based catalysts, where the HCHO intermediate was formed by dehydrogenation of methanol. This was also identified by other researchers [32,33], who found that CH_3OH is first dehydrogenated to HCHO followed by a nucleophilic attack of H_2O to form HCOOH, which is further decomposed to H_2 and CO_2 on Cu-Zn based catalysts. The calculation results based on density functional theory (DFT) also indicated that HCHO intermediate involves in the SRM reaction on Cu (111) and Pd (111) surface [34]. On Cu (111) surface, HCHO intermediate can be formed by dehydrogenation of methanol though the O—H bond scission at first and then, HCHO tends to react with hydroxyl by the dissociation of H_2O to form hydroxymethoxy, which is finally decomposed to CO_2. In contrast, on Pd (111) surface, HCHO intermediate can be formed via the C—H bond breaking at first and then, directly decomposed to CO and H_2. All these results indicate that for different catalysts, the intermediate species formed on their surfaces seems to be different. To understand the reaction pathway of SRM over metal-modified molybdenum carbide, in this study, the reaction intermediate species generated were investigated by using the TPSR approach, in which a mass spectroscopy was applied to detect the products on-line. The obtained data were analyzed and discussed.

2. Experimental

2.1. Catalysts preparation

The catalysts were synthesized with the same procedure described in our previous studies [11–13]. In short, the molyb-

denum carbide (β-Mo_2C) was synthesized by carburizing molybdenum oxide (MoO_3) using temperature programmed reduction (TPR) method with 20% CH_4/H_2 mixture. Subsequently, the as-prepared fresh sample was passivated at room temperature using a 1% O_2/Ar gas mixture. For preparation of metal modified molybdenum oxide (M-MoO_x) (M: Pt, Cu, and Ni), Firstly, aqueous solutions of $(NH_4)_6Mo_7O_{24}\cdot 4H_2O$ respectively mixed with $H_2PtCl_6\cdot 6H_2O$, $Cu(NO_3)_2\cdot 3H_2O$, $Ni(NO_3)_2\cdot 6H_2O$ under stirring for 4 h at first, and then the mixture solutions were continuously stirred at 80 °C until dried. After continuously dried at 110 °C overnight, the samples were calcined in air at 500 °C for 4 h. The obtained M-MoO_x precursors were carburized using the same method as that for preparation of β-Mo_2C. It is found that Pt-Mo_xC_y with a Pt/Mo molar ratio of 1.6/90(Pt-Mo_xC_y(1.6)) [11], Ni-Mo_2C with a Ni/Mo molar ratio of 1.6/98.4(Ni-Mo_2C(1.6))[11,12], Cu-Mo_2C with a Cu/Mo molar ratio of 10/90 (Cu- Mo_xC_y(10)) [13] showed the highest activity and stability for each metal-modified molybdenum oxide. In this study, these three kinds of catalysts were for TPSR.

2.2. Temperature programmed surface reaction (TPSR)

CH_3OH-TPSR and CH_3OH-H_2O-TPSR were respectively investigated in a quartz micro-reactor with an inner diameter of 6 mm. 100 mg passivated molybdenum carbide based catalyst was loaded in the reactor. Prior to the reaction, the catalyst was pretreated with 15% CH_4/H_2 at 590 °C for 2 h in order to reduce the surface oxide, and then the temperature was raised to 700 °C with a heating rate of 1 °C/min under Ar flow (50 cm^3/min) and remained at 700 °C for 2 h in order to remove the adsorbents on the catalyst surface, and finally the temperature was decreased to room temperature under Ar flow. TPSR was performed in 13% CH_3OH-Ar (50 cm^3/min) or 13% CH_3OH-13% H_2O-Ar (50 cm^3/min) gas flow, in which the reaction temperature was increased from the room temperature (RT) to 700 °C with a heating rate of 5 °C/min. The signal intensities of CO_2 (m/e = 44), CO (m/e = 28), CH_4 (m/e = 15), H_2 (m/e = 2), H_2O (m/e = 18), CH_3OH (m/e = 31), HCOOH (m/e = 46) and $HCOOCH_3$ (m/e = 60) were on-line monitored by mass spectroscopy (MS, BEL Mass, BEL Japan Inc.).

3. Results and discussion

3.1. Methanol decomposition pathway over β-Mo_2C surface

As stated above, in this study, TPSR is used to study the interaction between the reactants and catalyst surface. As shown in Fig. 1(a), for CH_3OH-TPSR over β-Mo_2C surface, one can see that the decomposition of CH_3OH starts at 205 °C, which is consistence with the result obtained in our previous study [11,12]. When the reaction temperature is increased to 420 °C, the methanol signal increases. This might be due to the coke formation from methanol dissociation at high temperature. Meanwhile, from Fig. 1(b), one can see that small amounts of two intermediate species, formic acid (HCOOH) and methyl-formate ($HCOOCH_3$), appear along with H_2, CH_4, CO_2 and CO. As reported by other researchers [28–32], for other kinds of catalysts, the surface of catalyst is always dominated by methoxy and formate groups, and methyl-formate usually appears in the product spectrum at high methanol surplus. Moreover, the formed methyl-formate can be further converted to formic acid (HCOOH), which can finally decompose to H_2 and CO_2. In this study, the results also indicate that the decomposition of methanol over β-Mo_2C catalyst surface also follows the methyl-formate ($HCOOCH_3$) intermediate species pathway, i.e., pathway II as indicated in Eqs. (3)–(5). Here, the formation of formic acid can be attributed to the conversion of dioxymethylene (H_2COO) as following [30]:
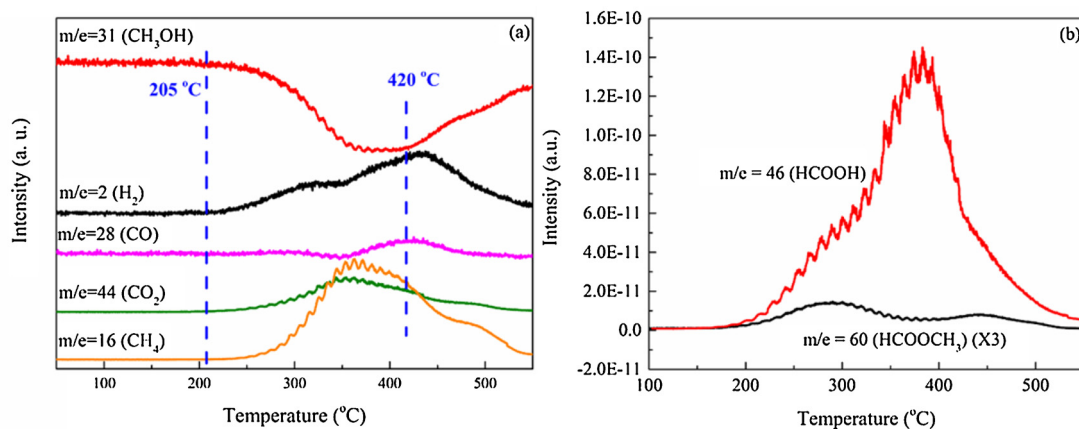
$$2H_2COO_{(a)} \rightarrow 2HCOO + H_2 \qquad (9)$$

Fig. 1. CH_3OH-TPSR profiles over β-Mo_2C catalyst surface.
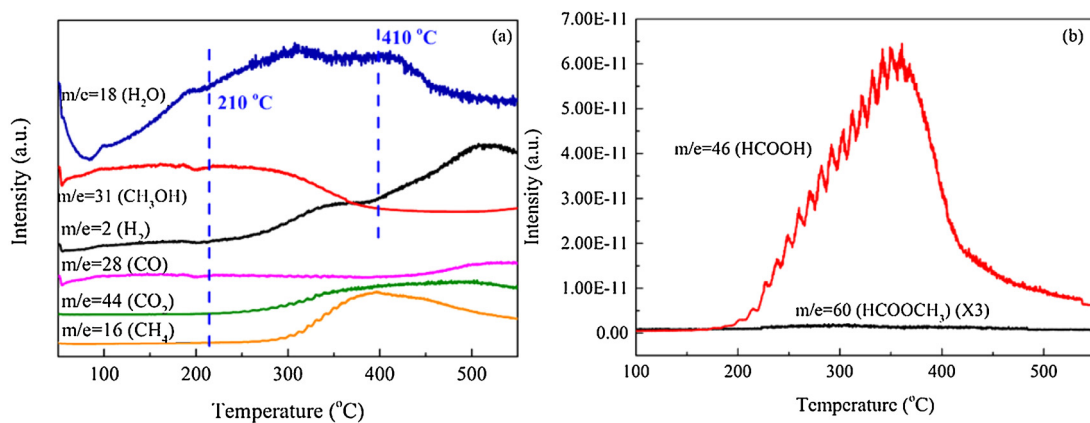

Fig. 2. CH_3OH-H_2O-TPSR profiles over β-Mo_2C catalyst surface.
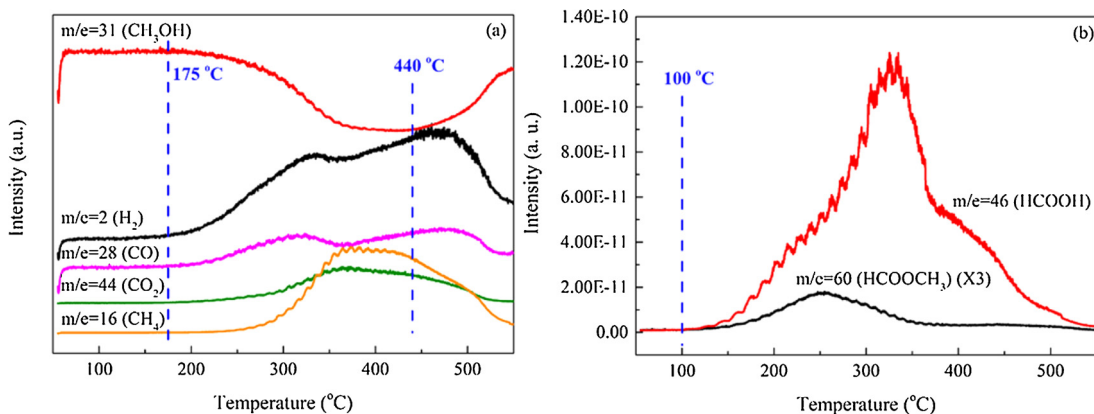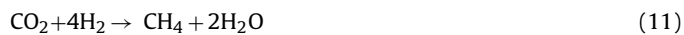

Fig. 3. CH_3OH-TPSR profiles over Ni-Mo_2C (1.6) catalyst surface.

Meanwhile, the formation of CO_2 and CH_4 in the outlet might be due to $HCOOCH_3$ decomposition, and another possibility is that CH4 may be derived from *methanation*, from the generated CO_2 and H_2 (Eq. (11)):

$$HCOOCH_3 \rightarrow CO_2 + CH \qquad (10)$$

$$CO_2 + 4H_2 \rightarrow CH_4 + 2H_2O \qquad (11)$$

It should be noted that the temperature for CO formation is higher than that for other species. As such, CO may be also derived from the decomposition of $HCOOCH_3$ (Eq. (12)), but it will compete with the formation of CO_2 and CH_4 (Eq. (10)). The other possible

way for CO formation may be from the reverse water gas shift reaction (Eq. (13)).

$$HCOOCH_3 \rightarrow CO + CH_3OH \qquad (12)$$

$$CO_2 + H_2 \rightarrow CO + H_2O \qquad (13)$$

3.2. SRM pathway over β-Mo_2C surface

Fig. 2 shows CH_3O H-H_2O-TPSR profiles over β-Mo_2C catalyst surface. One can see that the reaction starts at 210 °C, and with the reaction temperature increased to 410 °C, the signal of H_2O
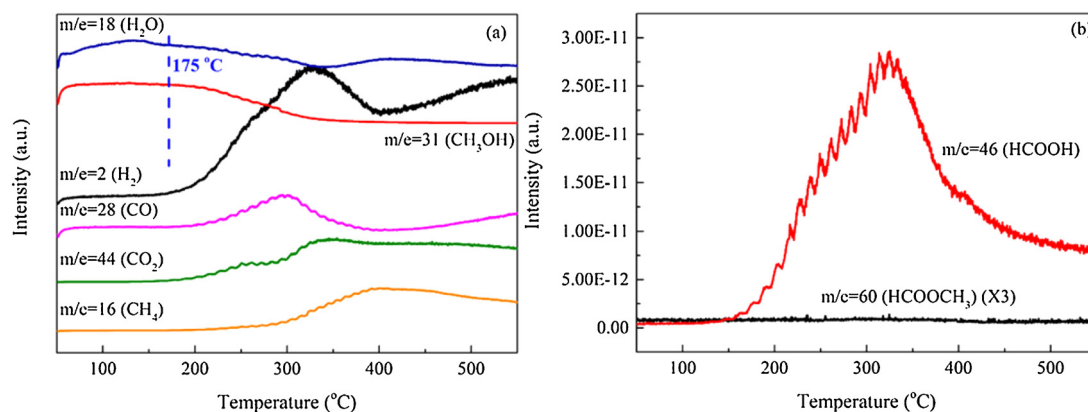
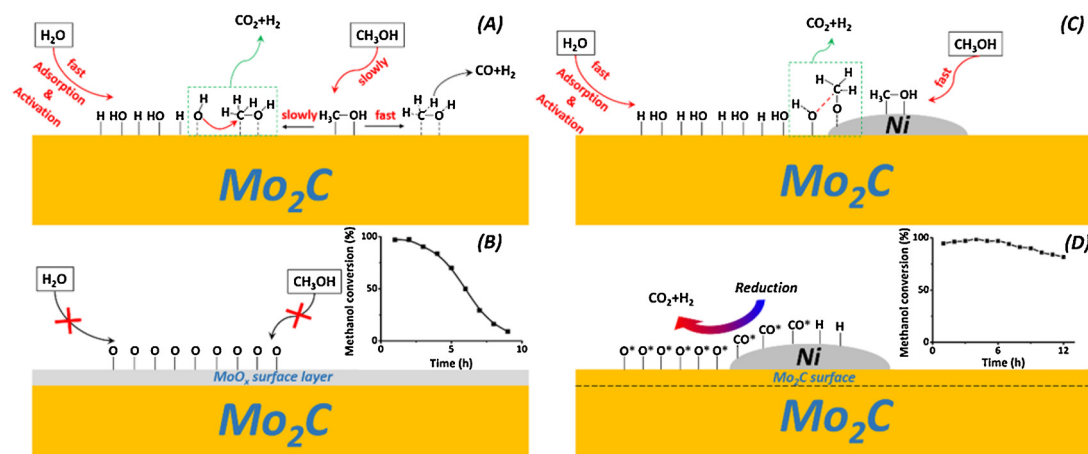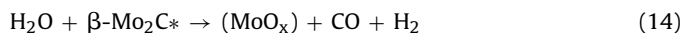**Fig. 4.** CH_3OH-H_2O-TPSR profiles over Ni-Mo_2C (1.6) catalyst surface.

Fig. 5. Schematic illustration of SRM reaction on catalyst surfaces ((A) and (B): β-Mo_2C surface; (C) and (D): Ni-modified Mo_2C surface) *: adsorbed species.

decreases sharply while that of H_2 increases, indicating that the β-Mo_2C surface could be oxidized by water (Eq. (14)) at high reaction temperatures (>400 °C).

$$H_2O + \beta\text{-}Mo_2C_* \rightarrow (MoO_x) + CO + H_2 \qquad (14)$$

Compared with Fig. 1, one can find that the intensity of CO signal decreases by the addition of H_2O. This is due to WGS reaction (Eq. (2)) occurring in the CH_3O H-H_2O system. On the other hand, based on Fig. 2(b), it is obvious that only trace of $HCOOCH_3$ can be detected, but the intermediate species of HCOOH still remains relatively high. In contrast, as shown in Fig. 1(b), methyl-formate can be easily detected in the case without steam. As such, it can be concluded that $HCOOCH_3$ can react with H_2O to generate HCOOH (Eq. (4)). Here, methyl-formate should be also the intermediate of methanol decomposition on the surface of catalyst, which could further react with H_2O in the reaction system. Therefore, for SRM reaction over β-Mo_2C catalyst surface, methyl-formate ($HCOOCH_3$) should be the intermediate species.

3.3. SRM reaction pathway over metal-modified molybdenum carbide surface

If compare Fig. 3 with Fig. 1, one can find that the start temperature for the methanol decomposition is decreased by modification of Ni on the molybdenum carbide catalyst surface, indicating that the dissociative adsorption of methanol molecule is enhanced by the loaded Ni metal, which is generally considered to be benefit for the hydrocarbon reforming reaction. On the other hand, if compare Fig. 4 with Fig. 2, one can see that the SRM reaction also
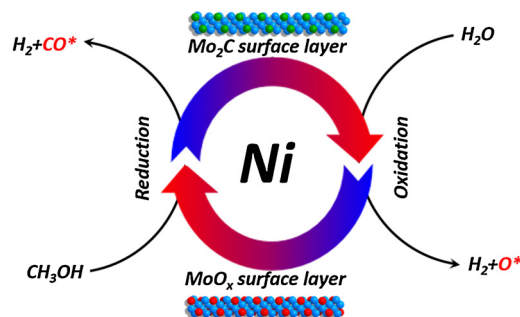

Fig. 6. Catalytic oxidation-reduction cycle over Ni-Mo_2C catalyst.

starts at lower temperature (175 °C) due to the modification of Ni on the molybdenum carbide catalyst surface. With the reaction temperature increased to high range (>400 °C), there is no obvious decrease of water signal (Fig. 4(a)). Also, correlated with β-Mo_2C-TPSR results, it can be found that the intermediate species on Ni-Mo_2C (1.6) catalyst surface is almost the same as that on pure β-Mo_2C surface. Therefore, the SRM reaction pathway on Ni-Mo_2C (1.6) is similar to that on the pure β-Mo_2C catalyst surface.

Based on our previous studies [11–14], the oxidation of Mo_2C with oxygen species is originated from the dissociation of H_2O on β-Mo_2C or metal-modified molybdenum carbide catalysts, and as such, the surface reaction mechanism can be assumed as illustrated in Fig. 5. As shown in Fig. 5(A) and (B), the rates of water adsorption and activation over β-Mo_2C catalyst surface are fast due to
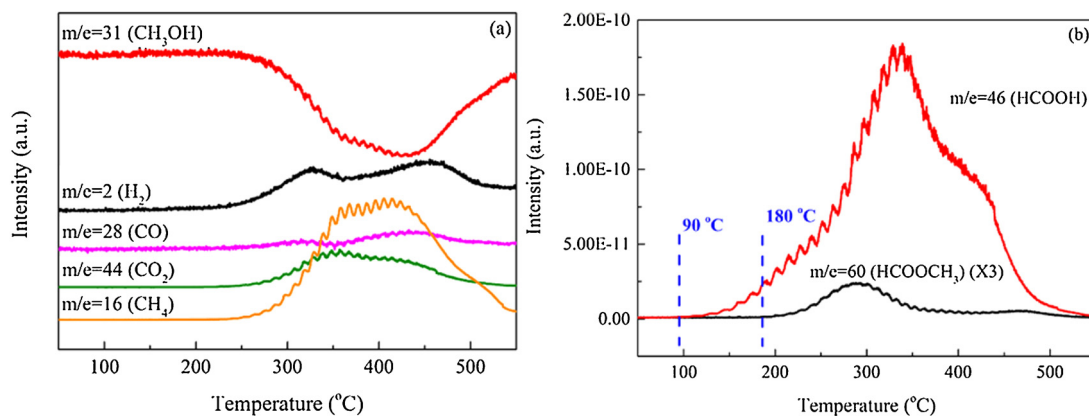
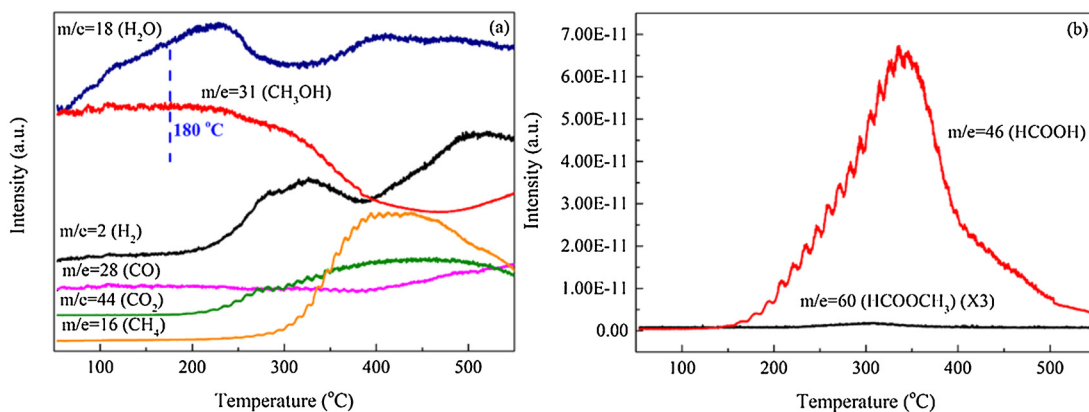**Fig. 7.** CH$_3$OH-TPSR profiles over Cu-Mo$_2$C (10) catalyst surface.

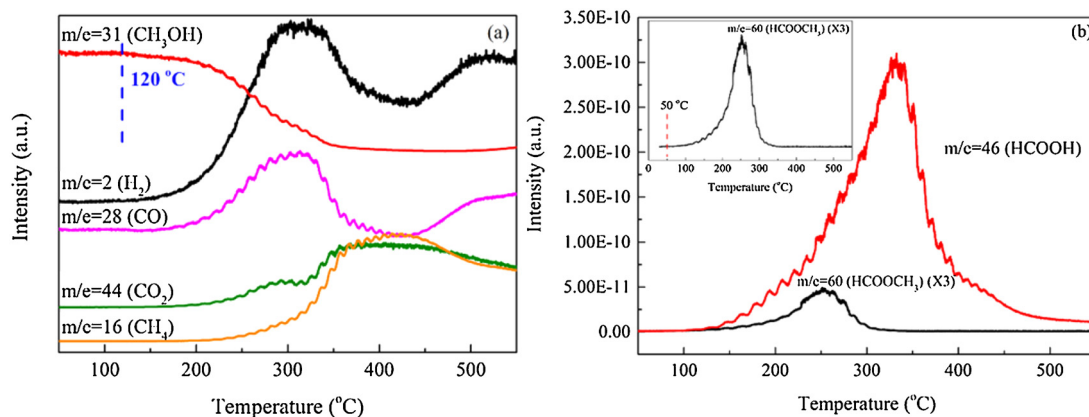**Fig. 8.** CH$_3$OH-H$_2$O-TPSR profiles over Cu-Mo$_2$C (10) catalyst surface.

Fig. 9. CH$_3$OH-TPSR profiles over Pt-Mo$_2$C (1.6) catalyst surface.

the reduced property of the molybdenum carbide surface. It should be noted that water serves as the oxide reactant here. In contrast, methanol is a relatively more reduced reactant and thus, the rates of methanol adsorption and dissociation should be much slower than water dissociation on the molybdenum carbide surface. However, the reaction pathway during SRM reaction is still ambiguous. As shown in Fig. 5(B), with the time on stream, the molybdenum carbide surface can be gradually oxidized by oxygen species from the dissociation of water molecule. Moreover, it should be noted that the surface oxygen species could hinder other reactant adsorption. However, when the metal such as Ni is loaded on the molybdenum carbide surface, Ni could accelerate the rate of methanol activa-

tion and dissociation and as a result, more reduced species i.e. CO* could be produced from methanol and the surface oxygen species generated from water could be reduced by CO* species, as shown in Fig. 5(C) and (D). In conclusions, the deactivation of β-Mo$_2$C catalyst during SRM reaction is due to that the reaction rate of water activation is faster than methanol dissociation. As such, the oxidized Mo species cannot be reduced by methanol. When metal such as Ni is loaded on the molybdenum carbide surface with suitable amount, the balance of oxidation and reduction rates can be achieved and an oxidation-reduction cycle shown in Fig. 6 could be established over it. That is why the activity and stability of molybdenum carbide are greatly promoted by doping some metals with proper amount.
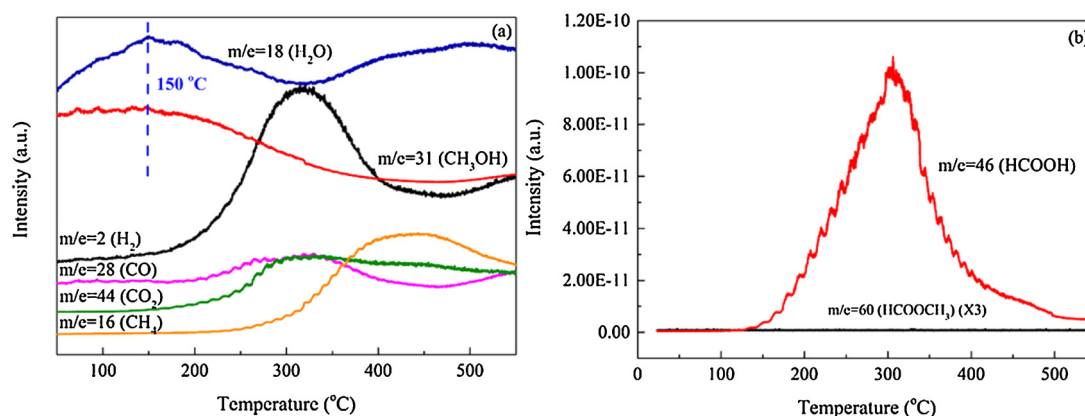
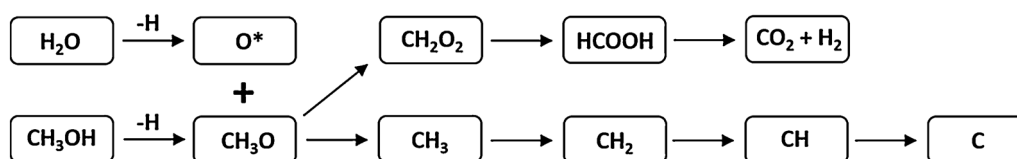**Fig. 10.** CH_3OH-H_2O-TPSR profiles over $Pt-Mo_2C$ (1.6) catalyst surface.

Fig. 11. Schematic diagram of SRM reaction pathway over $Cu-Mo_xC_y$ (10) catalyst surface (90–180 °C).

Table 1
The main features of $\beta-Mo_2C$, $Ni-Mo_2C$ (1.6), $Cu-Mo_2C$ (10) and $Pt-Mo_2C$(1.6).

	$\beta-Mo_2C$	$Ni-Mo_2C$ (1.6)	$Cu-Mo_2C$ (10)	$Pt-Mo_2C$ (1.6)
Metal oxidation states		Ni^{0}[a]	Cu^{0}[a]	Pt^{0}[a]
CH_3OH conversion(200 °C)[b]	3%	17%	64%	99%
Stability (h)	9	12	11	50
CH_3OH- TPSR reaction start temperature (°C)	205	175	90	120
CH_3OH-H_2O-TPSR reaction start temperature (°C)	210	175	180	150
Reaction intermediates	Formic acid and methyl-formate	Formic acid and methyl-formate	Methyl-formate	Methyl-formate

[a] Before test the catalysts were regenerated under 15% CH_4/H_2 gas flow.

[b] References [11–13].

Figs. 7 and 8 shows CH_3OH-TPSR and CH_3O H-H_2O-TPSR profiles over $Cu-Mo_2C$ (10) catalyst surface, respectively. One can see that the activation of methanol molecule over Cu modified molybdenum carbide catalyst starts at a temperature as low as 90 °C. Compared with the pure $\beta-Mo_2C$ catalyst, the activation temperature is greatly decreased. This indicates that the dissociative adsorption of methanol molecule can be greatly enhanced by the modification of Cu. Here, methanol molecule is considered to be mainly adsorbed on the Cu metal surface. On the other hand, as shown in Fig. 7(b), one can find that the methanol dissociation on the $Cu-Mo_xC_y$ (10) catalyst surface has two stages: one is at the reaction temperature range of 90–180 °C; the other is the reaction temperature over 180 °C. Especially, in the first stage, only HCOOH intermediate species appears, indicating that the activation of methanol molecule can be enhanced at lower temperature due to the modification of Cu species. Based on our previous study [13], the high activity and stability should be attributed to the formation of Cu^{I} species on the catalyst surface, which was detected by XPS analysis and the Auger Cu LMM spectra.

Similar as shown in Fig. 4, the results in Fig. 8 indicate that the water signal has no significant decrease. As mentioned above, the oxidation-reduction cycle shown in Fig. 6 should be also existed on the Cu modified molybdenum carbide catalyst surface.

Figs. 9 and 10 shows CH_3OH-TPSR and CH_3OH-H_2O-TPSR profiles over $Pt-Mo_xC_y$ (1.6) catalyst surface, respectively. It is obvious that the methanol activation temperature is decreased more

(50 °C). This indicates that the methanol molecule can be dissociated on Pt modified molybdenum carbide catalyst even at near the room temperature. Our previous study also showed that $Pt-Mo_xC_y$ (1.6) catalyst has high activity and stability for SRM reaction at low temperatures [14] and the results are consistence with those shown here. On the other hand, as shown in Fig. 10(a), the water signal also has no significant decrease. This also indicates that the resistance of oxidation of molybdenum carbide has been enhanced by the modification of Pt. Furthermore, one can see that for the SRM reaction over Pt modified molybdenum carbide catalyst, methyl-formate ($HCOOCH_3$) is also the intermediate species.

3.4. Reaction pathway

The main features of above catalysts can be summarized in Table 1. It shows that the metal modified Mo_2C catalysts have obviously improved when compared with the common $\beta-Mo_2C$ in catalytic activity and stability. Based on these TPSR results, one can conclude that the reaction pathway over molybdenum carbide and metal modified molybdenum carbide catalyst surface is the pathway II, i.e., though the methyl-formate ($HCOOCH_3$) intermediate species route. However, the methanol dissociation on the $Cu-Mo_xC_y$ (10) catalyst surface has two stages: one is at the reaction temperature range of 90–180 °C; the other is the reaction temperature over 180 °C. Therefore, the reaction pathway can be summarized in the following 2 figures:
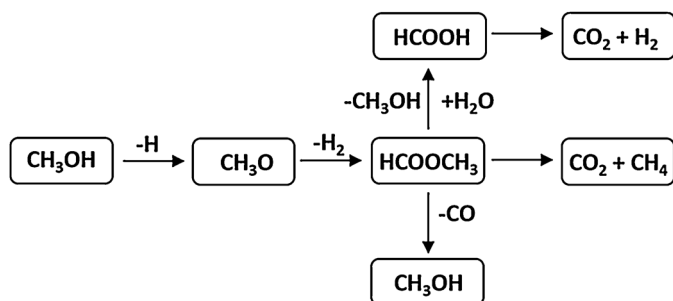
Fig. 12. Schematic diagram of SRM reaction pathway over β-Mo$_2$C, Ni-Mo$_2$C (1.6), Cu-Mo$_x$C$_y$ (10) and Pt-Mo$_x$C$_y$ (1.6) catalyst surfaces (>180 °C).

(i) SRM reaction pathway (formic acid (HCOOH) intermediate pathway) over Cu-Mo$_x$C$_y$ (10) in the temperature range of 90–180 °C (Fig. 11).

(ii) SRM reaction pathway(methyl-formate (HCOOCH$_3$) intermediate pathway) over β-Mo$_2$C, Ni-Mo$_2$C (1.6), Pt-Mo$_x$C$_y$ (1.6) and Cu-Mo$_x$C$_y$ (10) at a reaction temperature over180 °C (Fig. 12).

4. Conclusions

In this study, to understand the SRM reaction pathway over various metal-modified molybdenum carbide surfaces, reaction intermediate species generated during SRM reaction over the catalyst are investigated by using a temperature programmed surface reaction (TPSR) approach, in which a mass spectroscopy is applied to detect the products on-line. It is found that the reaction temperature affects the formation of different intermediate species over different catalysts. At the temperature lower than 180 °C, SRM reaction proceeds over Cu modified molybdenum carbide surface through formic acid (HCOOH) intermediate pathway, but at the temperature over 180 °C, the reactions over pure β-Mo$_2$C, Ni, Cu and Pt modified molybdenum carbide surfaces proceed through methyl-formate intermediate pathway. It is expected that these findings can help us understanding the mechanism on SRM reaction over molybdenum carbide based catalysts.

Acknowledgements

References

[1] S. Sá, H. Silva, L. Brandão, J.M. Sousa, A. Mendes, Catalysts for methanol steam reforming-a review, Appl. Catal. B: Environ. 99 (2010) 43–57.
[2] J. Papavasiliou, G. Avgouropoulos, T. Ioannides, Effect of dopants on the performance of CuO-CeO$_2$ catalysts in methanol steam reforming, Appl. Catal. B: Environ. 69 (2007) 226–234.
[3] G. Huang, B.J. Liaw, C.J. Jhang, Y.Z. Chen, Steam reforming of methanol over CuO/ZnO/CeO$_2$/ZrO$_2$/Al$_2$O$_3$ catalysts, Appl. Catal. A: Gen. 358 (2009) 7–12.
[4] S.D. Jones, H.E. Hagelin-Weaver, Steam reforming of methanol over CeO$_2$- and ZrO$_2$-promoted Cu-ZnO catalysts supported on nanoparticle Al$_2$O$_3$, Appl. Catal. B: Environ. 90 (2009) 195–204.
[5] S.C. Yang, W.N. Su, S.D. Lin, J. Rick, B.J. Hwang, Preparation of highly dispersed catalytic Cu from rod-like Cu O-CeO$_2$ mixed metal oxides: suitable for applications in high performance methanol steam reforming, Catal. Sci. Technol. 2 (2012) 807–812.
[6] C. Wang, M. Boucher, M. Yang, H. Saltsburg, M. Flytzani-Stephanopoulos, ZnO-modified zirconia as gold catalyst support for the low-temperature methanol steam reforming reaction, Appl. Catal. B: Environ. 154 (2014) 142–152.
[7] L. Yang, G.D. Lin, H.B. Zhang, Highly efficient Pd-ZnO catalyst doubly promoted by CNTs and Sc$_2$O$_3$ for methanol steam reforming, Appl. Catal. A: Gen. 455 (2013) 137–144.
[8] A. Haghofer, K. Föttinger, F. Girgsdies, D. Teschner, A. Knop-Gericke, R. Schlögl, G. Rupprechter, In situ study of the formation and stability of supported Pd$_2$Ga methanol steam reforming catalysts, J. Catal. 286 (2012) 13–21.
[9] N. Yi, R. Si, H. Saltsburg, M. Flytzani-Stephanopoulos, Steam reforming of methanol over ceria and gold-ceria nanoshapes, Appl. Catal. B: Environ. 95 (2010) 87–92.
[10] B. Halevi, E.J. Peterson, A. Roy, A. DeLariva, E. Jeroro, F. Gao, Y. Wang, J.M. Vohs, B. Kiefer, E. Kunkes, M. Havecker, M. Behrens, R. Schlogl, A.K. Datye, Catalytic reactivity of face centered cubic PdZnα for the steam reforming of methanol, J. Catal. 291 (2012) 44–54.
[11] Y. Ma, G. Guan, C. Shi, A. Zhu, X. Hao, Z. Wang, K. i Kusakabe, A. Abudula, Low-temperature steam reforming of methanol to produce hydrogen over various metal-doped molybdenum carbide catalysts, Int. J. Hydrogen Energy 39 (2014) 258–266.
[12] Y. Ma, G. Guan, P. Phanthong, X. Hao, W. Huang, A. Tsutsumi, K. Kusakabe, A. Abudula, Catalytic activity and stability of nickel modified molybdenum carbide catalysts for steam reforming of methanol, J. Phys. Chem. C 118 (2014) 9485–9496.
[13] Y. Ma, G. Guan, X. Hao, Z. Zuo, W. Huang, P. Phanthong, K. Kusakabe, A. Abudula, Highly-efficient steam reforming of methanol over copper modified molybdenum carbide, RSC Adv. 4 (2014) 44175–44184.
[14] Y. Ma, G. Guan, P. Phanthong, X. Li, J. Cao, X. Hao, Z. Wang, A. Abudula, Steam reforming of methanol for hydrogen production over nanostructured wire-like molybdenum carbide catalyst, Int. J. Hydrogen Energy 39 (2014) 18803–18811.
[15] S.S.Y. Lin, W.J. Thomson, T.J. Hagensen, S.Y. Ha, Steam reforming of methanol using supported Mo$_2$C catalysts, Appl. Catal. A: Gen. 318 (2007) 121–127.
[16] P. Liu, J.A. Rodriguez, Water-gas-shift reaction on molybdenum carbide surfaces: essential role of the oxycarbide, J. Phys. Chem. B 110 (2006) 19418–19425.
[17] R. Barthos, F. Solymosi, Hydrogen production in the decomposition and steam reforming of methanol on Mo$_2$C/carbon catalysts, J. Catal. 249 (2007) 289–299.
[18] J. Patt, D.J. Moon, C. Phillips, L. Thompson, Molybdenum carbide catalysts for water-gas shift, Catal. Lett. 65 (2000) 193–195.
[19] A. Széchenyi, F. Solymosi, Production of hydrogen in the decomposition of ethanol and methanol over unsupported Mo$_2$C catalysts, J. Phys. Chem. C 111 (2007) 9509–9515.
[20] Á. Koós, R. Barthos, F. Solymosi, Reforming of methanol on a K-promoted Mo$_2$C/Norit catalyst, J. Phys. Chem. C 112 (2008) 2607–2612.
[21] M. Nagai, A.M. Zahidul, Y. Kunisaki, Y. Aoki, Water-gas shift reactions on potassium- and zirconium-promoted cobalt molybdenum carbide catalysts, Appl. Catal. A: Gen. 383 (2010) 58–65.
[22] M. Nagai, A.M. Zahidul, K. Matsuda, Nano-structured nickel-molybdenum carbide catalyst for low-temperature water-gas shift reaction, Appl. Catal. A: Gen. 313 (2006) 137–145.
[23] M. Nagai, K. Matsuda, Low-temperature water–gas shift reaction over cobalt–molybdenum carbide catalyst, J. Catal. 238 (2006) 489–496.
[24] C. Shi, A. Zhang, X. Li, S. Zhang, A. Zhu, Y. Ma, C. Au, Ni-modified Mo$_2$C catalysts for methane dry reforming, Appl. Catal. A: Gen. 431 (2012) 164–170.
[25] A. Zhang, A. Zhu, B. Chen, S. Zhang, C. Au, C. Shi, In-situ synthesis of nickel modified molybdenum carbide catalyst for dry reforming of methane, Catal. Commun. 12 (2011) 803–807.
[26] E. Santacesaria, S. Carra, Kinetics of catalytic steam reforming of methanol in a CSTR reactor, Appl. Catal. B: Environ. 5 (1983) 345–358.
[27] W. Luo, A. Asthagiri, Density functional theory study of methanol steam reforming on Co(0001) and Co(111) surfaces, J. Phys. Chem. C 118 (2014) 15274–15285.
[28] B. Frank, F. Jentoft, H. Soerijanto, J. Kröhnert, R. Schlögl, R. Schomäcker, Steam reforming of methanol over copper-containing catalysts: influence of support material on microkinetics, J. Catal. 246 (2007) 177–192.
[29] S. Lin, D. Xie, H. Guo, First-principles study of the methyl formate pathway of methanol steam reforming on PdZn(1 1 1) with comparison to Cu(1 1 1), J. Mol. Catal. A: Chem. 356 (2012) 165–170.
[30] N. Yi, R. Si, H. Saltsburg, M. Flytzani-Stephanopoulos, Steam reforming of methanol over ceria and gold-ceria nanoshapes, Appl. Catal. B: Environ. 95 (2010) 87–92.
[31] N. Takezawa, N. Iwasa, Steam reforming and dehydrogenation of methanol: difference in the catalytic functions of copper and group VIII metals, Catal. Today 36 (1997) 45–56.
[32] J.P. Breen, J.R. Ross, Methanol reforming for fuel-cell applications: development of zirconia-containing Cu-Zn-Al catalysts, Catal. Today 51 (1999) 521–533.
[33] T. Shishido, Y. Yamamoto, H. Morioka, K. Takehira, Production of hydrogen from methanol over Cu/ZnO and Cu/ZnO/Al$_2$O$_3$ catalysts prepared by homogeneous precipitation: steam reforming and oxidative steam reforming, J. Mol. Catal. A: Chem. 268 (2007) 185–194.
[34] X.K. Gu, W.X. Li, First-Principles study on the origin of the different selectivities for methanol steam reforming on Cu(111) and Pd(111), J. Phys. Chem. C 114 (2010) 21539–21547.